2005

Flow Patterns Generated by Oblate Medusan Jellyfish: Field Measurements and Laboratory Analyses

John O. Dabiri
California Institute of Technology

Sean Colin
Roger Williams University, scolin@rwu.edu

John H. Costello
Providence College

Morteza Gharib
Roger Williams University

Recommended Citation
Dabiri, J. O., Colin, S. P., Costello, J. H., and Gharib, M. 2005. Flow Patterns Generated by Oblate Medusan Jellyfish: Field Measurements and Laboratory Analyses. *J. Exp. Biol.* 208: 1257-1269.

The Journal of Experimental Biology 208, 1257-1265
Published by The Company of Biologists 2005
doi:10.1242/jeb.01519

Flow patterns generated by oblate medusan jellyfish: field measurements and laboratory analyses

John O. Dabiri[1,*], Sean P. Colin[2], John H. Costello[3] and Morteza Gharib[1]

[1]*Bioengineering and Graduate Aeronautical Laboratories, California Institute of Technology, Mail Code 301-46, Pasadena, CA 91125, USA*, [2]*Biology and Marine Biology, Roger Williams University, MNS 241, Bristol, RI 02809, USA* and [3]*Biology, Providence College, Providence, RI 02918, USA*

*Author for correspondence (e-mail: jodabiri@caltech.edu)

Accepted 31 January 2005

Summary

Flow patterns generated by medusan swimmers such as jellyfish are known to differ according the morphology of the various animal species. Oblate medusae have been previously observed to generate vortex ring structures during the propulsive cycle. Owing to the inherent physical coupling between locomotor and feeding structures in these animals, the dynamics of vortex ring formation must be robustly tuned to facilitate effective functioning of both systems. To understand how this is achieved, we employed dye visualization techniques on scyphomedusae (*Aurelia aurita*) observed swimming in their natural marine habitat. The flow created during each propulsive cycle consists of a toroidal starting vortex formed during the power swimming stroke, followed by a stopping vortex of opposite rotational sense generated during the recovery stroke. These two vortices merge in a laterally oriented vortex superstructure that induces flow both toward the subumbrellar feeding surfaces and downstream. The lateral vortex motif discovered here appears to be critical to the dual function of the medusa bell as a flow source for feeding and propulsion. Furthermore, vortices in the animal wake have a greater volume and closer spacing than predicted by prevailing models of medusan swimming. These effects are shown to be advantageous for feeding and swimming performance, and are an important consequence of vortex interactions that have been previously neglected.

Key words: jellyfish, *Aurelia aurita*, flow pattern, flow patterns, vortex rings, jet propulsion.

Introduction

Medusan swimmers propel themselves forward *via* periodic bell contractions, which act to decrease the volume of their subumbrellar cavity and jet water out of the oral end of their bell. Described as jet propulsion, prevailing models of this process focus on the fluid efflux that emerges during bell contraction: a toroidal volume of rotating fluid known as the power stroke starting vortex ring (Fig. 1).

Any vortex formation that may occur during the recovery stroke of the propulsive cycle is neglected in existing models of the swimming process (e.g. Daniel, 1983; Colin and Costello, 2002; McHenry and Jed, 2003). Therefore interactions between adjacent vortex rings in the wake have been previously examined with the assumption of a uniform train of starting vortex rings in the animal wake, each with identical rotational sense.

Weihs (1977) used a quasi-steady model of such a vortex ring train to conclude that substantial thrust augmentation can occur – up to 150% relative to a steady jet – if the vortex rings are spaced sufficiently close together (i.e. $C/(B+D)$ is small; see Fig. 1). The thrust benefit arises from the induced downstream velocity of the vortex ring train on each of its members. Interestingly, the flow pattern depicted by Ford et al. (see fig. 5 in Ford et al., 1997) for the oblate jellyfish *Chrysaora quinquecirrha* shows a train of closely spaced vortex rings.

The proximity of the wake vortex rings to each other and to the swimming animal as measured by Ford et al. (1997) is unexpected given the tendency of individual vortex rings to rapidly propagate away from the flow source due to self-induced velocity (Lamb, 1932) and convection by any jet-like flow that is present behind each ring. An estimate by Daniel (1983) of the medusan wake vortex ring train using these assumptions predicts a spacing of 10 vortex ring radii between adjacent rings. This result agrees with a physical intuition for the formation of successive vortex rings with identical rotational sense, but is incompatible with the experimental measurements of Ford et al. (1997).

Given difficulties in quantitatively measuring vortex ring properties using particle tracking methods, one cannot make *a priori* preference for either the measurements of Ford et al. (1997) or the model estimate of Daniel (1983). An experimental re-examination of both the measured flow patterns of Ford et al. (1997), and the assumptions leading to the model of Daniel (1983) is necessary to clarify this issue.

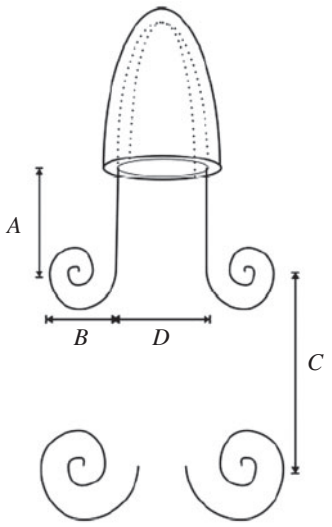

Fig. 1. Schematic of a jetting medusa with vortex rings in the wake. Vortex rings are shown in cross section. *A*, jet length; *B*, vortex ring core diameter; *C*, vortex ring spacing; *D*, jet diameter.

The importance of this effort is underscored by the heavy reliance on both the model of Daniel (1983) and observations of power stroke vortex ring formation to develop generalized dynamical models of medusan swimming (e.g. Colin and Costello, 2002; McHenry and Jed, 2003).

Of further concern is the fact that existing models of medusan behavior make little association between swimming and the prey capture mechanisms required for feeding. Yet, a clear relationship between swimming and feeding has been documented for a variety of medusae, notably larger oblate forms (Costello and Colin 1994, 1995).

Owing to the inherent physical coupling between the locomotor and feeding structures in medusae, it is important to investigate how the generated flow patterns can efficiently meet the demands of both systems. Fluid motions must be heavily utilized in the process of capturing prey and transporting it to feeding surfaces, while maintaining a capability to generate thrust for swimming. The physical mechanisms whereby the observed vortex ring structures accomplish both tasks are currently unknown.

The objective of this paper is to elucidate the nature and utility of flow structures generated by oblate swimming medusae. In order to understand how flow contributes to both thrust production and feeding mechanisms, we utilized flow visualization to qualitatively and quantitatively examine flow patterns surrounding the oblate scyphomedusa *Aurelia aurita* L. swimming in its natural marine habitat.

Specifically, we observed the motion of fluorescent dye markers injected at several locations around the bells of swimming *A. aurita* medusae. These field observations eliminate the need for an imposed flow current, as is necessary in typical laboratory tanks that house medusae (i.e. kreisel facilities). The swimming kinematics and dynamics measured by this method should be more relevant to animal behavior in the marine water column than those achieved by any type of laboratory tank. Further, the use of a continuous dye marker instead of discrete prey for particle tracking simplifies the identification of large-scale fluid structures in the flow, such as vortex rings. In addition, the three dimensional nature of the flow (in the absence of significant vortex stretching) does not limit the effectiveness of the dye marker technique, as is the case with particle tracking. By observing vortex dynamics in the wake and fluid–structure interactions near the medusa bell, the role of the observed flow structures is clarified.

Materials and methods

Video measurements

Field data was collected from a marine lake (145 hectares, maximum depth 46 m) on the island of Mljet, Croatia located in the Adriatic Sea (Lat: 42.75°N, Long: 17.55°E) during July 2003. All of the video was taken in shallow water (<20 m) by a Scuba diver using natural light. Video recordings followed the methods of Costello et al. (1998), whereby medusae were recorded at 30 frames s^{-1} on miniDV videotape using a Sony DCR VX2000 camera with a zoom lens contained within an Amphibico underwater housing. A second diver injected 20 μl pulses of concentrated fluorescene dye into the fluid at specific locations around the medusae. This second diver was located to the side of the medusae at 90° to the orientation of the video camera. Both divers took care to avoid disturbing the fluid around the medusa being videoed. The dye made any disturbances by the divers obvious allowing these shots to be excluded from the analysis. The length of the pipette tip used to administer the dye (approximately 4 cm) was used as a scale in later analysis.

Several hours of videotape were recorded in which medusae were observed swimming both in large groups and in isolation. The swimming kinematics were qualitatively consistent throughout the observations using the dye technique. In order to achieve more quantitative results, a subset of the full video database was analyzed in greater detail.

Kinematic analyses

Select recordings of animal swimming in the field were collected for further laboratory analysis. For kinematic analyses, sequences of recorded swimming motions of two medusae were chosen according to visibility of the medusa subumbrellar surface, motion in planes parallel to the camera, separation from other medusae, and sufficient dye marker in the flow. In addition, the upper and lower limits of animal size were sought, to facilitate comparisons of fluid dynamic and geometric scaling. The larger medusa in the kinematic analyses is an order of magnitude larger than the small medusa (10.2 cm maximum bell diameter *vs* 3.6 cm maximum bell diameter, or 22 times larger by volume).

Video recordings of up to five successive swimming contractions of each animal were analyzed using the algorithm of Dabiri and Gharib (2003). Between 10 and 20 control points along the subumbrellar surface of each medusa were tracked

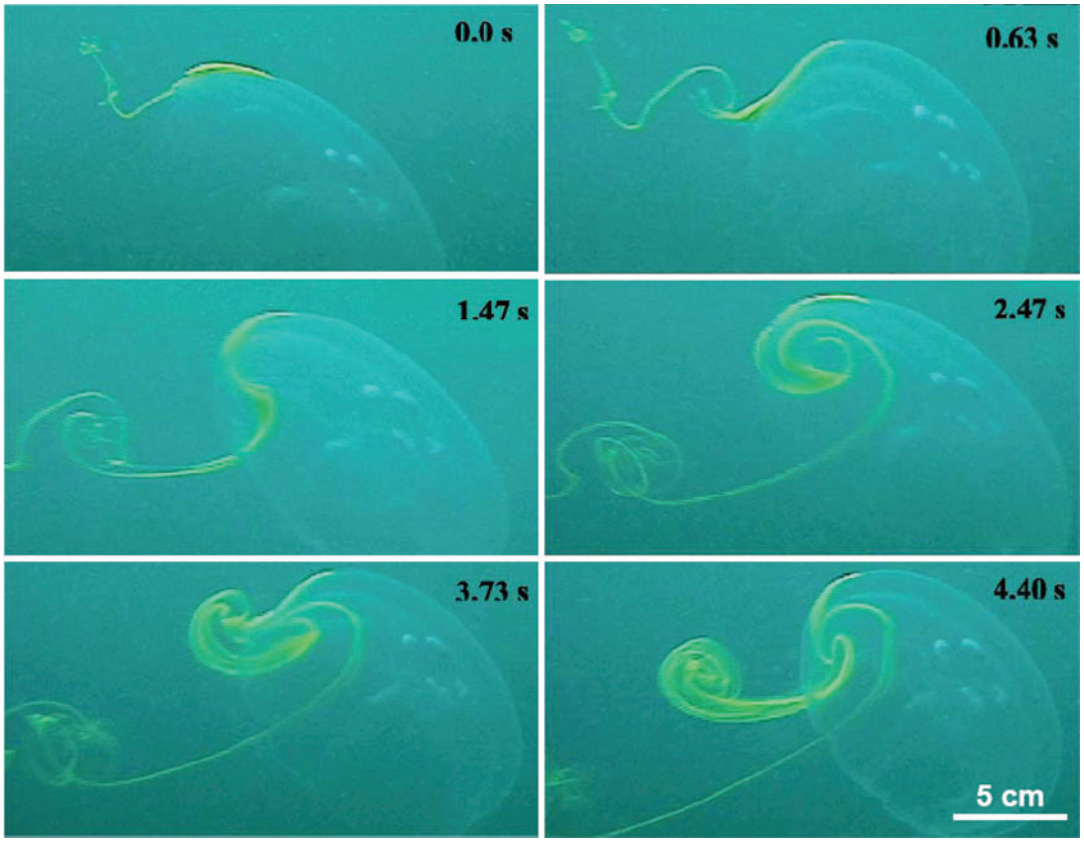

Fig. 2. Video sequence of vortex ring formation during two swimming cycles of *Aurelia aurita*. At 0 and 2.47 s the bell is relaxed and fully expanded. Frames at 0.63 and 3.73 s show the contraction phase and the formation of the starting vortex. Frames at 1.47 and 4.40 s show the relaxation phase, the trailing starting vortex and the formation of the stopping vortex. The frame at 2.47 shows a fully developed stopping vortex in the subumbrellar cavity.

during swimming motions to generate a computational reconstruction of the medusae kinematics. The entire subumbrellar surface was clearly visible through the transparent mesoglea in each of the selected frames, and any fluorescent dye carried inside the medusa bell further improved the resolution of the interface location.

In addition to measuring the shape of the bell, the properties of the formed vortex rings were analyzed. Specifically, the volume of each vortex ring and the inter-ring spacing of the vortex ring train in the animal wake were measured. The physical extent of each vortex ring was measured based on the distribution of the dye marker in the flow.

The kinematic analyses include only frames in which the animals are swimming parallel to the image plane of the camera. Hence, the orientation of the vortex rings can be assumed to be such that the ring axis is also parallel to the image plane. To calculate the volume of the visible toroidal vortex rings, we therefore require only measurements of the diameter across the toroid (*B*+*D* in Fig. 1) and the diameter of the vortex core (*B* in Fig. 1).

Important caveats associated with this measurement technique are discussed in the following section. Each set of measurements is presented conservatively, with an uncertainty calculated as the maximum difference between any individual measurement and the average of the set. This metric is used in lieu of the standard deviation (S.D.), since the S.D. tends to underestimate the data spread for relatively small sample sizes such as those studied here (Freedman et al., 1998).

Strategies for dye marker interpretation

Despite the convenience of a passive dye marker for qualitative flow visualization, there are important limitations to the technique. First, although all of the dye labels fluid, not all of the fluid is labeled by dye. Therefore if one desires to track the evolution of a fluid structure such as a vortex ring using the passive dye marker, the visible labeled structure may be smaller than the actual fluid structure. When identifying vortex rings in the flow, the dye-labeled ring represents a lower bound on the size of the vortex.

Secondly, the diffusion coefficient of dye markers such as that used in these experiments (fluorescene) is substantially less than the diffusion coefficient of fluid vorticity (i.e. rotation and shear), as measured by the kinematic viscosity of water ($\sim 10^{-2}$ cm^2 s^{-1}). Hence, regions of compact vorticity such as the wake vortex rings will tend to spread by diffusion at a rate faster than can be observed in the dye. Again, the result is that

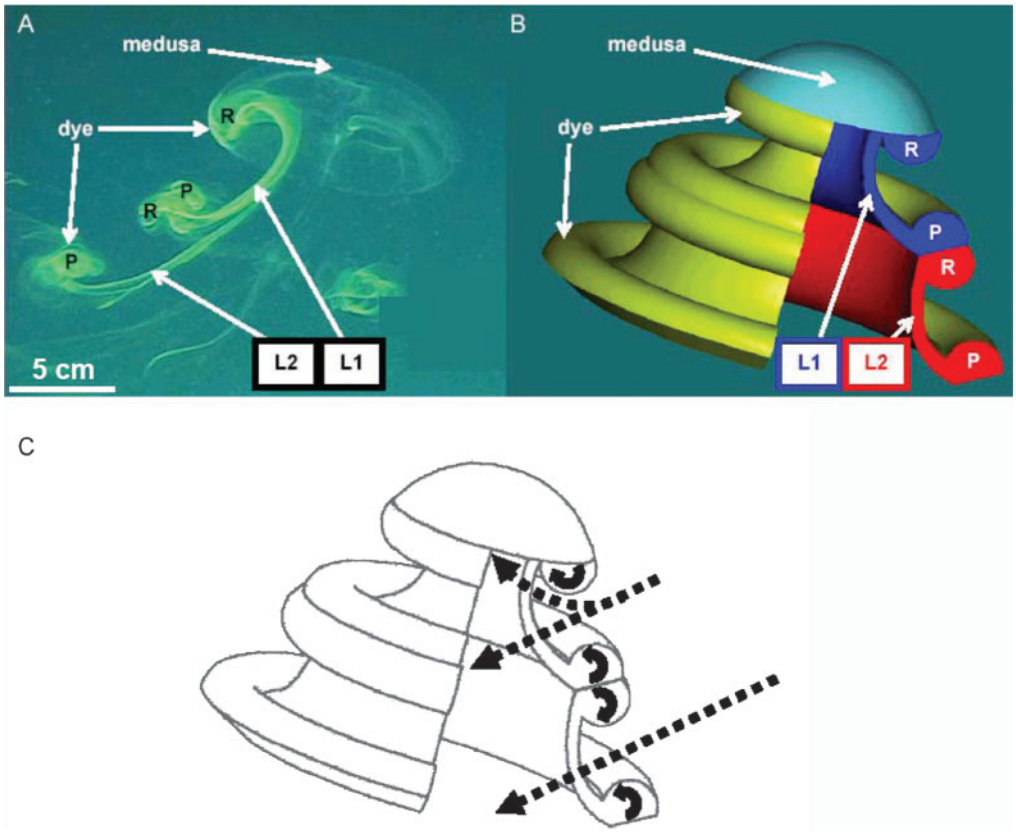

Fig. 3. Kinematics of the starting, stopping and co-joined lateral vortex structures. (A) Image of medusa vortex wake. (B) Corresponding schematic of medusa vortex wake. P, power stroke starting vortex ring; R, recovery stroke stopping vortex ring; L1/L2, adjacent lateral vortex superstructures. (C) Flow paths in vortex wake. Solid arrows indicate directions of vortex rotation; broken arrows, flow induced by vortex rotation.

the visibly labeled structure may be smaller than the actual fluid structure. Consequently, all of our estimates of vortex ring volume are conservative values.

Our strategy was to exploit these limitations by assuming that the measurements represent a lower bound on the size of the vortex rings. The effects of a departure from the lower bound case can be inferred from the available data.

Results

Vortex formation process

The swimming cycle of *Aurelia aurita* consists of a bell contraction phase (i.e. power stroke) and a bell relaxation phase (i.e. recovery stroke). Observations of fluorescent dye that was injected into the fluid outside the bell along the bell margin of swimming *A. aurita* revealed that the two phases of the swimming cycle interacted with the surrounding fluid to form distinct vortex rings at separate locations relative to the bell.

During the power stroke the bell contracted and initiated the formation of a starting vortex ring. The starting vortex ring induced a motion of fluid originating from regions both inside the subumbrellar volume and outside the bell *via* entrainment of ambient fluid. The induced motion was oriented at an angle away from the bell margin and toward both the central axis of the bell and downstream (Fig. 2). At maximum contraction, the starting vortex was fully developed and traveling away from the medusa.

As the bell relaxed, a stopping vortex was formed inside the subumbrellar cavity. The stopping vortex induced a motion of fluid originating from outside the bell and toward the subumbrellar cavity. Consequently, as the subumbrellar

Table 1. *Relationship between starting vortex ring kinematics and dynamics*

Parameter	Thrust	Efficiency
Vortex ring volume	+	+
Vortex ring spacing	–	–
Jet ratio *A*/*D*	+	–

Both thrust and efficiency increase in direct proportion with vortex ring volume. By contrast, thrust and efficiency decrease with increasing vortex spacing due to diminished inter-ring interactions. For a fixed volume of ejected fluid, the thrust increases with jet ratio *A*/*D*, at the expense of efficiency.

Trends are based on the assumption of negligible vortex formation during the recovery stroke. + indicates a direct relationship and – an inverse relationship (cf. Weihs, 1977; Krueger and Gharib, 2003).

volume increased with bell relaxation, the stopping vortex served to refill the subumbrellar volume with fluid from outside the bell.

The stopping vortex remained in the subumbrellar cavity during the beginning of the contraction phase of the next swimming cycle. As the bell contracted, a part of the stopping vortex ring was ejected from the subumbrellar cavity and interacted with the starting vortex of the new cycle. In the interaction, a portion of the fluid from the stopping vortex co-joined with the starting vortex ring, completing formation of the downstream lateral vortex superstructure. The kinematics of the starting, stopping and co-joined lateral vortex structure are illustrated in Fig. 3. Although the schematic in Fig. 3B suggests a clear distinction between power and recovery stroke vortices in the wake, the two components actually become highly amalgamated because of fluid mixing. This process makes the individual vortices increasingly difficult to distinguish as the wake develops.

There are several important observations to be made from the qualitative analysis of the formation and interaction of the starting and stopping vortex rings during swimming cycles. First, throughout the swim cycle, from the onset of the contraction phase through the relaxation phase, there is a continual flow of water that originates external to the bell and passes adjacent to the bell margin before entering the bell. During the contraction, the flow contributes to the fluid in the starting vortex ring but during bell relaxation it contributes to the fluid in the stopping vortex ring. Second, during a sequence of propulsive cycles we observed that the stopping vortex ring from the preceding lateral vortex structure persists in the bell and contributes to the formation of the subsequent starting vortex (Fig. 2). A complex interaction occurs as the starting vortex ring grows and the previous stopping vortex is convected downstream away from the bell margin. The interaction appears to increase the volume but decrease the velocity of the starting vortex ring, *via* cancellation of starting vortex vorticity by the preceding stopping vortex ring of opposite rotational sense (cf. Lim and Nickels, 1995). As a result of this interaction, the vortex ring volume and vortex ring spacing of swimming oblate medusae do not relate to thrust in the manner predicted for a unidirectional pulsed jet of fluid through an orifice (i.e. Table 1). Existing models for the time-dependent thrust neglect recovery stroke vortex formation altogether and therefore do not apply to these medusae.

The interaction between starting and stopping vortices described above tends to increase the total momentum of each wake vortex. This is because the mass of each wake vortex increases (i.e. the starting and stopping vortex masses combine in the wake) to a greater degree than the wake vortex velocity decreases *via* vorticity cancellation. The effect of vorticity cancellation is limited because it is a viscosity-dependent process that occurs only at the interface between the starting and stopping vortices (Shariff and Leonard, 1992).

Dye injected into the middle of the subumbrellar volume is not ejected directly outwards during bell contraction but instead spreads laterally along the subumbrellar surface of the bell. All of the dye leaves the subumbrellar cavity at the bell margin. However, it takes the medusa several swim cycles to eject all of the dye from the subumbrellar region. No fluid is ever directly ejected from the central subumbrellar region. In fact, there is always a net flow into the subumbrellar cavity in the central portion trailing to the bell. This is due to the direction of rotation of the stopping vortex ring in this region (Fig. 3).

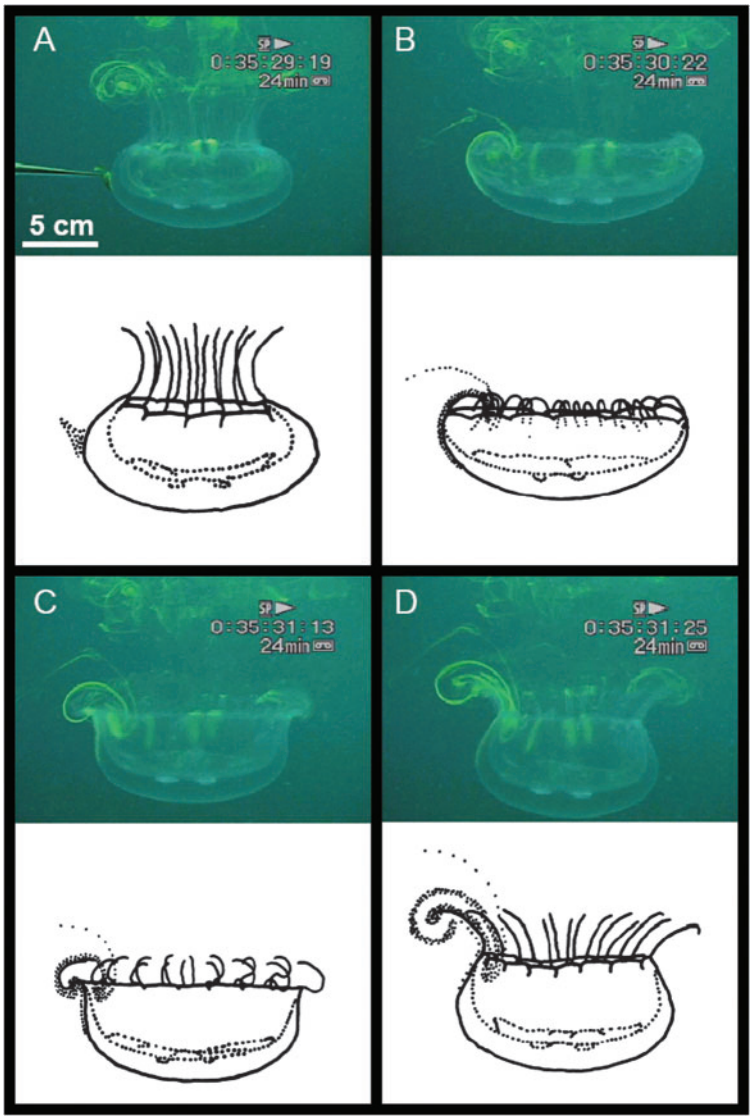

Fig. 4. Video sequence and schematic of fluorescent dye relative to the tentacles of *Aurelia aurita* during a swimming cycle. (A) The dye placed along the exumbrella. (B) The bell expanding and drawing the dye through the tentacles toward the subumbrellar cavity as part of the stopping vortex. (C,D) The bell contracting and expelling the dye along the tentacles as part of the starting vortex.

Tentacle positioning

Throughout the pulsation cycle the tentacles of *A. aurita* were primarily located in vortex rings (Fig. 4). At the beginning of the contraction phase they were in the subumbrellar cavity in the stopping vortex ring. As the bell contracted the tentacles become entrained in the starting vortex ring, which oriented the tentacles in a trailing position. At the end of the contraction phase and the onset of the relaxation phase, the tentacles became entrained in the stopping vortex ring which drew them back up into the subumbrellar cavity.

Vortex ring kinematic measurements

Several important aspects of the fully formed wake vortices were investigated quantitatively. Wake vortices visualized with dye markers allow for quantitative evaluation of thrust production mechanisms. In this regard, an important variable is the volume of each wake vortex ring relative to the volume of fluid ejected by the medusa. Although the results of the preceding section suggest a more complex relationship between swimming thrust and vortex kinematics than has been previously appreciated, we can anticipate that, for a fixed swimming frequency (and corresponding characteristic flow velocity), swimming thrust will maintain a direct relationship with vortex volume (cf. Daniel, 1983). We cannot neglect the fact that the characteristic flow velocity is reduced by vorticity cancellation between the starting and stopping vortices. However, as mentioned previously, this effect is limited in the present case. Therefore volume measurements provide the most useful index of swimming thrust in the present study.

The volume contained by the bell at full contraction and relaxation was measured using the subumbrellar surface profiles obtained from the video analysis. The difference between these two values gives the volume of fluid ejected. The ratio of wake vortex ring volume Ω_w to ejected fluid volume Ω_b was relatively insensitive to animal size: 3.09±0.35 for the smaller animal, and 3.57±0.40 for the larger. Two primary effects contribute to the large volume of the wake vortex rings relative to the volume of fluid ejected. First of these is the presence of the stopping vortex ring, which is created from fluid external to the bell. This stopping vortex is complexed with the starting vortex ring of the subsequent lateral vortex to create each wake vortex ring. Secondly, both starting and stopping vortex ring formation processes involve substantial entrainment of ambient fluid from outside the bell.

Given the vortex ring kinematic measurements, we can also determine the inter-ring spacing in the wake vortex ring train. In both medusae, the wake vortex rings are very closely spaced. The inter-ring spacing is 1.36±0.08 ring radii in the smaller medusa and 1.06±0.06 ring radii in the large medusa.

Table 2 presents the measurements of vortex ring kinematics in dimensional form.

Table 2. *Dimensional values of kinematics measurements for selected medusae*

Parameter	Smaller medusa	Larger medusa
Vortex ring volume (cm^3)	62±7	1213±131
Vortex ring radius (cm)	3.3±0.3	7.9±0.5
Vortex ring spacing (cm)	4.6±0.5	10.7±0.8

Smaller and larger medusae have maximum bell diameters of 3.6 cm and 10.2 cm, respectively.

Discussion

Implications for medusan swimming behavior

Dye studies of the swimming oblate medusa *Aurelia aurita* demonstrated the formation of two vortex rings during each bell pulsation cycle. As expected, we observed the formation of a starting vortex ring during bell contraction but, unexpectedly, we observed the formation of a stopping vortex ring during bell relaxation and an interaction of these two vortices to form a lateral vortex superstructure in the wake of the medusa. The discovery of co-joined starting-stopping vortex ring structures in these oblate medusan wakes requires modification of prevailing jet-propulsion models that assume medusan wakes to consist of a simple train of discrete single-sign vortex rings.

The observation of stopping vortex ring formation is not entirely new. It is well known from experiments on vortex ring formation by mechanical apparatus that such structures appear at the end of fluid ejection – hence their title (e.g. Didden, 1979). The source of vorticity for these structures is the interaction between flow external to the vortex ring generator and its outer surface. In a swimming medusa, this corresponds to the interaction of external fluid with the expanding bell margin. The strength of the stopping vortex ring will be directly proportional to the velocity of external fluid past the bell (Didden, 1979), and is therefore coupled to the swimming speed of the animal and the local kinematics of the bell margin.

The presence of such a pronounced stopping vortex ring has profound consequences on thrust production and estimates of thrust. As mentioned, it substantially increases the volume of fluid in each wake vortex ring, Ω_w, relative to the volume of fluid from inside the bell Ω_b. For laboratory-generated vortex rings in the absence of background flow, Dabiri and Gharib (2004) found that approximately one third of the vortex ring volume originates from ambient fluid external to the jet flow. If we assume that the medusa stopping vortex ring is approximately the same size as the starting vortex ring (a reasonable assumption based on the dye visualizations), then a one-third entrained fluid fraction in each starting and stopping vortex ring will lead to a ratio of wake vortex ring volume to ejected fluid volume equal to 3, i.e.

$$\frac{\Omega_w}{\Omega_b} = \frac{\Omega_{start}+\Omega_{stop}}{\Omega_b} = \frac{\frac{3}{2}\Omega_b+\frac{3}{2}\Omega_b}{\Omega_b} = 3\ . \qquad (1)$$

Comparing this value with the present measurements, it appears the two effects that we have identified as contributing to the relatively large wake vortex ring volume are sufficient to explain the observations. It is prudent to note that the starting and stopping vortex volumes are indeed additive in equation

1, despite the fact that the vortices possess opposite rotational sense. This is because the volume of each individual vortex is conserved despite the dynamical influences of vorticity cancellation and induced velocity effects (Lim and Nickels, 1995).

Since the swimming thrust increases directly with wake vortex volume (for a fixed swimming frequency and characteristic flow velocity), the presence of a stopping vortex ring has the potential to greatly increase swimming thrust. Based on the present measurements, the swimming thrust from the co-joined wake vortex ring motif would be larger than a steady jet of bell fluid by more than a factor of three. However, the estimated thrust advantage by this mechanism would probably be mitigated in practice by a lower convective velocity for the wake vortex rings relative to a steady jet flow, because of vorticity cancellation effects presented earlier.

The starting-stopping vortex interactions could also potentially increase swimming thrust *via* the velocity field that the opposite-sign vortices induce on one another, in a manner similar to the effect experienced by vortices near solid surfaces (i.e. ground effect; Rayner and Thomas, 1991; Shariff and Leonard, 1992). Quantitative visualization techniques will be necessary to validate the existence of such an effect in these animals.

The swimming efficiency is difficult to define for these animals because the flow is highly unsteady, and there is no clear protocol for including the relaxation phase in such a calculation. However, we can anticipate an increase in swimming efficiency, given that a Froude-type calculation predicts higher efficiencies for cases in which fluid is transported in high volume and at low velocity, as is observed here (Vogel, 1994).

The above findings demonstrate that the effect of the complex vortex ring wake structure must be considered in any realistic model of oblate medusan swimming. Specifically, it is insufficient to estimate thrust production by swimming oblate medusae using measurements of bell kinematics (e.g. Colin and Costello, 2002; McHenry and Jed, 2003) without a wake vortex ring analysis, since the stopping vortex is fully formed from the beginning of the bell motion. Also, the fluid inside the bell is not at rest (with respect to the medusa) when bell contraction is initiated, as must be assumed in a paddle model of the bell kinematics (e.g. McHenry and Jed, 2003).

In addition to the relationship between individual vortex kinematics and thrust, the relation between inter-vortex ring spacing and thrust may also differ from established models of jet propulsion. Similar to the observations of Ford et al. (1997), we observed reduced downstream propagation of wake vortices and, hence, a very close spacing between adjacent wake vortex rings. The flow visualization methods employed here enable us to resolve the apparent conflict between measurements and physical intuition for the dynamics of individual vortex rings. Reduced downstream propagation of the wake vortices is the result of vorticity cancellation. For rapid self-induced motion of vortex rings from a flow source it is fundamental that the vortex rings possess a single sign of rotation (Lamb, 1932). In the event that opposite-sign rotation is present, vorticity cancellation will occur in the vortex ring structure, resulting in a vortex ring with weaker self-induced motion. Oblate medusae encounter vorticity cancellation by two means as the flow pattern is being generated. First, the motion of each starting vortex toward the bell axis of symmetry leads to vorticity cancellation with mirror-image portions of the vortex on the opposite side of the bell margin. This effect is enhanced by motion of the bell margin toward the axis of symmetry during bell contraction. This type of vorticity cancellation commences almost immediately after bell contraction is initiated.

Secondly, as previously mentioned, the stopping vortex of the preceding lateral vortex structure interacts with each newly forming starting vortex ring. This additional vorticity cancellation occurs in proportion to the strength of the stopping vortex. Vorticity cancellation by this means can occur almost immediately after bell contraction because of the close proximity of the vortex structures carrying opposite-signed vorticity. The combined result of these processes is reduced downstream propagation of wake vortices and, hence, a very close spacing between adjacent wake vortex rings.

Although it is tempting to further suggest that the thrust benefits from close inter-ring spacing predicted by Weihs (1977) may be applicable to the dynamics of these medusae, one must remember that the derivation of Weihs (1977) assumes a train of single-sign vortex rings. Whether or not a similar benefit could be derived for the co-joined wake vortex rings studied here is a question still to be resolved.

Implications for medusan feeding behavior

Vortex formation and the use of accompanying induced flows are fundamentally important to feeding by swimming *A. aurita*. Medusae that feed as cruising predators, such as *A. aurita*, are highly dependent on locally generated flow currents to capture prey (Costello and Colin, 1994, 1995; Sullivan et al., 1994; Ford et al., 1997). For these animals, it is beneficial to generate flow regimes that increase encounter rates with prey. The stopping and starting vortex rings and the lateral vortex superstructure generated by *A. aurita* during swimming serve this role. First, both the starting and the stopping vortices entrain fluid from outside the bell throughout the pulsation cycle. This fluid is drawn past the bell margin toward the tentacles that are positioned in the starting vortex during bell contraction and the stopping vortex during bell relaxation (Fig. 4). Since the starting and stopping vortex rings entrain fluid during both the bell contraction and relaxation, respectively, *A. aurita* is able to use the full pulsation cycle for prey capture. Second, as discussed, the two vortex rings interact, enabling the starting vortex ring to entrain a greater volume of fluid than could be entrained by simplified jet flow. Therefore, medusae that generate starting and stopping vortices during swimming are able to process a large volume of water with each pulse. Finally, the prey entrained by the swimming medusae propagate away from the bell at a reduced rate because of the rotational flow of the wake vortex rings.

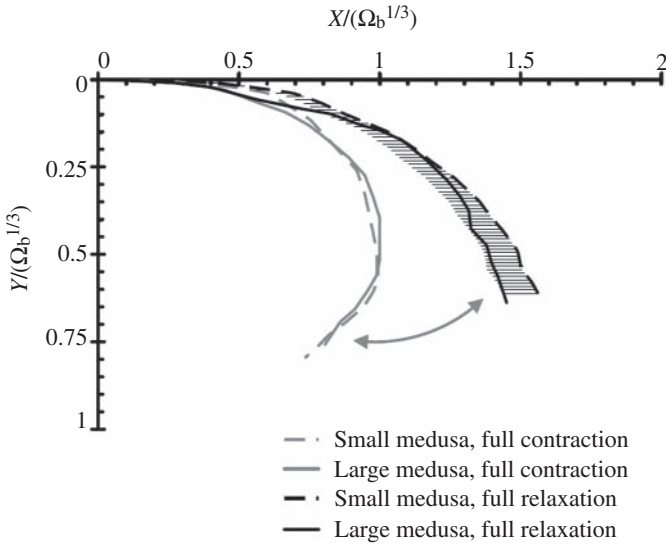

Fig. 5. Medusa bell shape profiles normalized by volume of ejected bell fluid Ω_b. Broken lines, small medusa; solid lines, large medusa; gray lines, full bell contraction; black lines, full bell relaxation. Horizontal bars denote measurement uncertainty.

These observed structures differ considerably from the jet-propulsion flow model (Fig. 1) in which the flow structures take the form of a uniform slug with minimal fluid entrainment. Consequently, the flow structures of swimming oblate medusae, such as *A. aurita*, have the potential to greatly increase encounter rates with prey relative to the flow structures of jet-propulsion.

The reduction in wake vortex ring propagation away from the bell should be amplified at higher swimming speeds, because the strength of the stopping vortex (used for vorticity cancellation) possesses direct proportionality to the fluid velocity past the bell (cf. Didden, 1979). The combined effect is a feeding mechanism that uses both bell contraction and relaxation productively for prey capture while being passively tuned for a range of swimming speeds. These flows provide potentially powerful mechanisms for prey encounter with the medusae.

The present dye visualization methods are insufficient to conclusively validate the existence of the passive fluid dynamic tuning mechanisms hypothesized here. However, future work using methods of quantitative velocimetry (e.g. digital particle image velocimetry; Willert and Gharib, 1991) will enable the direct measurements of starting and stopping vortex strength that are necessary to solidify these conclusions.

Implications for prolate medusae

Colin and Costello (2002) suggested that oblate and prolate medusae differ in their dependence on jet propulsion for thrust generation. Specifically, they concluded that prolate medusae display a strong jet flow component in the wake, whereas oblate species are dominated by vortex ring formation. Hence the results of the present study are primarily applicable to oblate forms. In several respects, however, our results may be relevant to prolate medusae.

The most important effect to recognize is that any accelerated jet with flow separation from a circular orifice and sufficiently large Reynolds number can form a vortex ring. Cantwell (1986) computed that the minimum Reynolds number required for vortex ring formation is approximately six. This is well below the swimming regime of medusan swimmers, both prolate and oblate (Gladfelter, 1973; Colin and Costello, 2002). We can therefore expect that prolate medusae will also experience vortex ring formation.

A primary difference between the wake of a prolate swimmer and that of an oblate form, however, lies in the duration of fluid ejection, as measured by the formation time (A/D; see Fig. 1). In laboratory experiments, Gharib et al. (1998) demonstrated that when the formation time exceeds a value of four, the leading vortex ring at the front of the fluid discharge stops growing and pinches off from the remaining fluid discharge behind it. In the swimming medusae, several additional parameters become important, such as temporal variation in the bell diameter and swimming speed (Krueger et al., 2003; Dabiri and Gharib, 2005). These factors will probably affect the ratio, changing it from the nominal value of four. Nonetheless, we can expect the physical principles to remain unchanged. Oblate medusae tend to eject fluid with small A/D ratios, thereby avoiding both pinch-off of the leading vortex ring and formation of a trailing jet flow. This leads to the observed dominance of vortex ring structures in the wake of oblate swimmers. By contrast, prolate medusae will tend to eject fluid with larger A/D ratios, leading to a substantial presence of jet flow behind the leading vortex rings in the flow. The difference in these ratios appears to be consistent with the different foraging strategies of the two forms. The low formation numbers of oblate forms suggest that their mode of propulsion may be more efficient, which is consistent with their cruising strategy (Table 1). Conversely, larger A/D ratios in prolate forms are consistent with their roles as ambush predators that periodically require large thrust generation, perhaps at the expense of swimming efficiency.

Colin and Costello (2002) show that the dominant presence of jet flow in prolate medusae makes them more amenable to models based on jet flow such as that of Daniel (1983). However, one cannot neglect to also examine the vortex ring formation that will occur early during bell contraction in prolate medusae. Some form of the co-joined wake vortex ring structures observed in the present study may also appear in the wakes of a variety of medusae, particularly those with intermediate bell morphologies between prolate and oblate. Further examination of wake structure and thrust generation will be necessary to properly model the dynamic swimming behavior of these animals.

A note on fluid dynamic and geometric scaling

One aim of this work has been to demonstrate the consistency of the observed flow patterns over a wide range of medusae sizes. If the fluid dynamical effects are insensitive to

geometric scaling – as we have seen here – then the kinematics of bell motion that dictate the fluid dynamics should also be scale invariant. We demonstrate this effect straightaway, by plotting the shape profile for the smaller and larger medusae at full bell contraction and relaxation in coordinates normalized by the cube root of the ejected bell fluid volume, $\Omega_b^{1/3}$ (Fig. 5). The cube root of the volume is used rather than the volume itself so that the normalized coordinates are dimensionless, thereby facilitating comparison across the full range of animal sizes. Consistent with the arguments presented in this paper and the findings of McHenry and Jed (2003), the bell kinematics are very similar, despite the order of magnitude difference in the volumes of the subjects. A similar examination should be made for other species of medusae, to determine the generality of the fluid dynamic and geometric scaling sensitivities observed here.

This research is supported by National Science Foundation Grants OCE-0116236 (to J.H.C.) and CTS-0309671 (to M.G.). We gratefully acknowledge helpful comments and suggestions from M. S. Gordon and two anonymous reviewers of this manuscript. We also acknowledge the support of the Ministry of Education, Science and Sport of the Republic of Slovenia, the Ministry of Science, Education and Sport of the Republic of Croatia and the University of Dubrovnik (Croatia).

References

Cantwell, B. J. (1986). Viscous starting jets. *J. Fluid Mech.* **173**, 159-189.

Colin, S. P. and Costello, J. H. (2002). Morphology, swimming performance, and propulsive mode of six co-occurring hydromedusae. *J. Exp. Biol.* **205**, 427-437.

Costello, J. H. and Colin, S. P. (1994). Morphology, fluid motion and predation by the scyphomedusa *Aurelia aurita*. *Mar. Biol.* **121**, 327-334.

Costello, J. H. and Colin, S. P. (1995). Flow and feeding by swimming scyphomedusae. *Mar. Biol.* **124**, 399-406.

Costello, J. H., Klos, E. and Ford, M. D. (1998). In situ time budgets of the scyphomedusae *Aurelia aurita*, *Cyanea* sp., and Chrysaora *quinquecirrha*. *J. Plankt. Res.* **20**, 383-391.

Dabiri, J. O. and Gharib, M. (2003). Sensitivity analysis of kinematic approximations in dynamic medusan swimming models. *J. Exp. Biol.* **206**, 3675-3680.

Dabiri, J. O. and Gharib, M. (2004). Fluid entrainment by isolated vortex rings. *J. Fluid Mech.* **511**, 311-331.

Dabiri, J. O. and Gharib, M. (2005). Starting flow through nozzles with temporally variable exit diameter. *J. Fluid Mech.* In press.

Daniel, T. L. (1983). Mechanics and energetics of medusan jet propulsion. *Can. J. Zool.* **61**, 1406-1420.

Didden, N. (1979). On the formation of vortex rings: rolling-up and production of circulation. *Z. Angew Math Phys.* **30**, 101-116.

Ford, M. D., Costello, J. H., Heidelberg, K. B. and Purcell, J. E. (1997). Swimming and feeding by the scyphomedusa *Chrysaora quinquecirrha*. *Mar. Biol.* **129**, 355-362.

Freedman, D., Pisani, R. and Purves, R. (1998). *Statistics*. New York: W. W. Norton.

Gharib, M., Rambod, E. and Shariff, K. (1998). A universal time scale for vortex ring formation. *J. Fluid Mech.* **360**, 121-140.

Gladfelter, W. G. (1973). Comparative analysis of locomotory systems of medusoid cnidaria. *Helgoland. Wiss. Meer.* **25**, 228-272.

Krueger, P. S., Dabiri, J. O. and Gharib, M. (2003). Vortex ring pinchoff in the presence of simultaneously initiated uniform background co-flow. *Phys. Fluids* **15**, L49-L52.

Krueger, P. S. and Gharib, M. (2003). The significance of vortex ring formation to the impulse and thrust of a starting jet. *Phys. Fluids* **15**, 1271-1281.

Lamb, H. (1932). *Hydrodynamics*. Cambridge: Cambridge University Press.

Lim, T. T. and Nickels, T. B. (1995). Vortex Rings. In *Fluid Vortices*. Kluwer Academic Publishers.

McHenry, M. J. and Jed, J. (2003). The ontogenetic scaling of hydrodynamics and swimming performance in jellyfish (*Aurelia aurita*). *J. Exp. Biol.* **206**, 4125-4137.

Rayner, J. M. V. and Thomas, A. L. R. (1991). On the vortex wake of an animal flying in a confined volume. *Phil. Trans. R. Soc. B* **334**, 107-117.

Shariff, K. and Leonard, A. (1992). Vortex rings. *Annu. Rev. Fluid Mech.* **24**, 235-279.

Sullivan, B. K., Garcia, J. R. and Klein-MacPhee, G. (1994). Prey selection by the scyphomedusan predator *Aurelia aurita*. *Mar. Biol.* **121**, 335-341.

Vogel, S. (1994). *Life in Moving Fluids*. Princeton: Princeton University Press.

Weihs, D. (1977). Periodic jet propulsion of aquatic creatures. *Forts. Zool.* **24**, 171-175.

Willert, C. E. and Gharib, M. (1991). Digital particle image velocimetry. *Exp. Fluids* **10**, 181-193.